

Final Draft
of the original manuscript:

Erickson, G.M.; Krick, B.A.; Hamilton, M.; Bourne, G.R.; Norell, M.A.;
Lilleodden, E.; Sawyer, W.G.:

**Complex Dental Structure and Wear Biomechanics in
Hadrosaurid Dinosaurs**

In: Science (2012) American Association

DOI: 10.1126/science.1224495

Complex Hadrosaurid Dinosaur Teeth Retain Tribological Properties Revealing Sophisticated Biomechanics

Gregory M. Erickson,^{1*} Brandon A. Krick,² Matthew Hamilton,² Gerald R. Bourne,³ Mark A. Norell,⁴ Erica Lilleodden,⁵ W. Gregory Sawyer²

¹Department of Biological Science, Florida State University, Tallahassee, FL 32306-4295, USA.

²Department of Mechanical and Aerospace Engineering, University of Florida, Gainesville, FL

32611, USA. ³Department of Metallurgical and Materials Engineering, Colorado School of

Mines, Golden, CO 80401. ⁴Division of Paleontology, American Museum of Natural History,

New York, NY 10024, USA, ⁵Institute of Materials Research, Materials Mechanics, Helmholtz-

Zentrum Geesthacht, Geesthacht, Germany.

Mammalian grinding dentitions are composed of four major tissues that differentially wear, creating coarse surfaces for pulverizing tough plants and liberating nutrients.

Although such dentition evolved repeatedly in mammals (e.g. horses, bison, elephants), a similar innovation occurred much earlier (~85 ma) within the duck-billed dinosaur group Hadrosauridae, fueling their 35 million year occupation of Laurasian mega-herbivorous niches. How this complexity was achieved is unknown, as reptilian teeth are generally two-tissue structures that presumably lack biomechanical attributes for grinding. Here we show that hadrosaurids broke from the primitive reptilian archetype and evolved six-tissue dental composition that is among the most sophisticated known. Three-dimensional wear models incorporating fossilized wear properties reveal how these tissues interacted for grinding and ecological specialization.

Hadrosaurids were the dominant large herbivores of Late Cretaceous Europe, Asia, and North America (1). Gut and fecal contents show that these gregarious, facultative bipeds (Fig. 1A) with broad duck-like bills grazed on horsetail, fern, and primitive angiosperm groundcover, and browsed on conifers (2). These tough plants, laden with siliceous phytoliths and/or exogenous grit that left their teeth scoured with wear striae (1), were pulverized using dentitions consisting of columns of developing and functional teeth with flattened horse and bison-like grinding surfaces (3, 4) (Fig. 1B-D). It's likely that exploitation of these food resources, that were presumably inaccessible to their forbearers with shearing teeth (5-7; Fig. 1E), facilitated the extensive hadrosaurid radiation (8, 9).

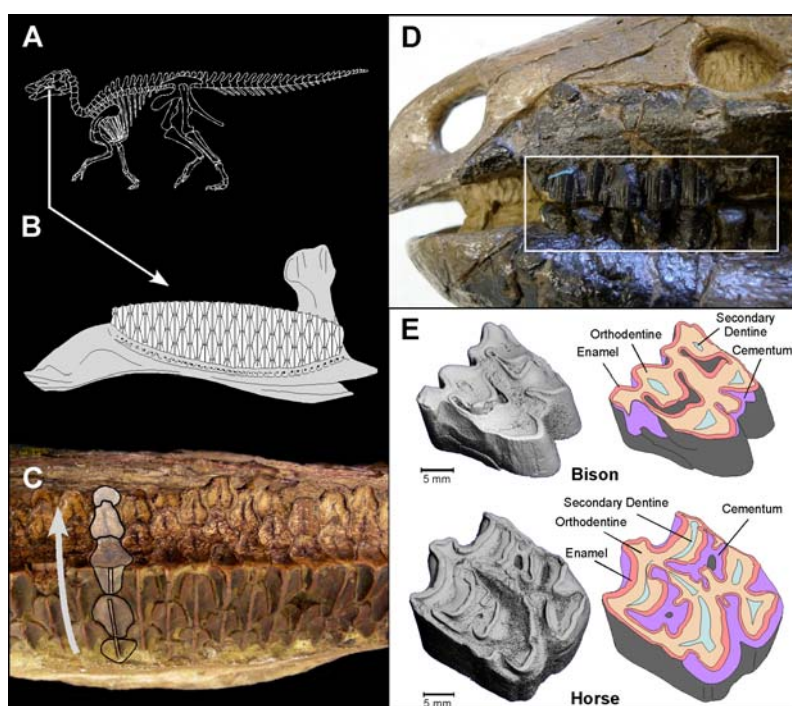


Fig. 1. Dental comparisons. (A) Hadrosaurid skeleton (*Edmontosaurus*). (B) Dental battery showing developing teeth (lingual). (C) *Edmontosaurus* dental battery showing progression of developing teeth and the grinding surface with teeth in various wear stages. (D) Ungulate grinding molars showing four-tissue composition. (E) Hadrosaurid outgroup condition (*Thescelosaurus*) possessing individual, shearing teeth at each position.

Traditional models of hadrosaurid chewing surfaces have included only the primitive reptilian (Sauria) dental tissues enamel (hard hypermineralized material) and orthodentine

(“dentine”; soft bone-like tissue) (3, 4) (Fig. 2A). According to those models, file-like crests and basins formed due to differential wear resistance as the teeth moved across the chewing surface (6) (Fig. 1C).

This two-tissue model contrasts with what we see in more complex mammalian grinding teeth (10-14) (Fig 1E). In mammals, major tissues, besides enamel and orthodentine, include soft secondary dentine (that forms a lower tier within basins sealing the pulp cavity to prevent abscesses), and coronal cementum (a derived root attachment tissue that migrates onto the crowns reducing stress on the brittle crests by transmitting loads among tissues).

The current model of hadrosaurid dental architecture is simplistic, lacking both crest-supporting and abscess-preventative tissues. Furthermore enamel is shown as present only in the leading teeth in the lower batteries (Fig. 2A), thereby leaving no hard tissues to form subsequent crests (Fig. 2B). Finally, conspicuous features are unaccounted for including, 1) granular material between teeth and filling pits within basins, 2) slicing planes on leading edge teeth, and 3) raised branched and linear ridges within the basins (15) (Fig. 2, B and C).

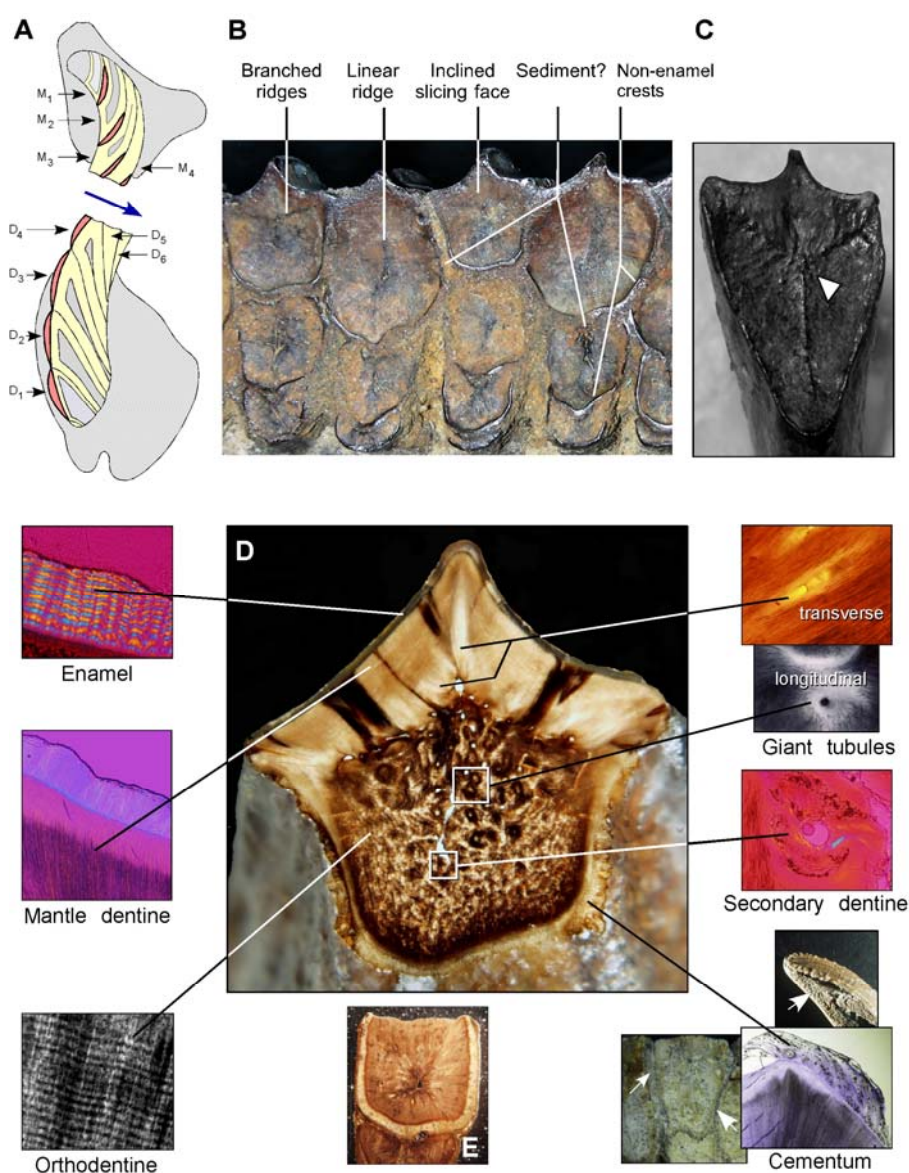


Fig. 2. Hadrosaurid dental organization. (A) Frontal section of jaws depicting just enamel (red) and “dentine” (yellow) tooth composition (3, 4), with no enamel layers across the lower chewing surface. The upper (maxillary) teeth and lower (dentary) teeth were drawn at various angles (1) across one another. Tooth developmental stages are numbered in the upper ($M_{\#}$) and lower ($D_{\#}$) jaws. (Worn teeth were shed every 45-80 days from each column [7]; up to 1,880/year across the dentition [17].) (B) Unexplained features on an *Edmontosaurus* chewing surface. (C) *Hadrosaurus* tooth with Y-shaped ridges (arrow). (D) Sections through *Edmontosaurus* teeth showing tissue types. Their presence and configurations vary throughout individual teeth. For instance, the roots (E), which become exposed, lack giant tubules. Note: coronal cementum (arrows) on the sides of a tooth crown, and on the chewing surface.

How was mammal-like grinding achieved in hadrosaurid dinosaurs? We provide the answers by, 1) characterizing tissue compositions and chewing surface morphologies in hadrosaurids and outgroup taxa, 2) mechanically testing the tissues for wear relevant attributes that, 3) are used in a tribological (study of wear) model to reveal the biomechanics of grinding surface formation, and 4) summarizing these findings in an evolutionary context.

Comprehensive phylogenies for the Hadrosauridae (8) (fig. S1; Table S1) and Ornithischia (16) were used to identify 27 specimens representing dental variation throughout the ornithopodan radiation. The tissue compositions were determined from intact batteries and transversely-sectioned teeth using dissecting and/or polarizing microscopy (17). Epoxy casts of worn chewing surfaces were made and the morphologies digitally captured using Laser Scanning Confocal Microscopy and Micro-Computerized Tomography (fig. S2).

Relative values for tissue wear rates (a direct measure of material removal), and hardnesses (resistance of a solid to permanent deformation when loaded and a proxy for wear rates) are the most pertinent properties for determining how individual dental tissues contribute to whole-tooth abrasive wear (18, 19). Yet they previously have not been recovered from fossils, but should be present. Tissue material properties are commonly recovered from dried modern teeth (20) that are analogous to well-preserved fossils, since apatite mineral content is the major determinant of dental tissue hardnesses (21). In a feasibility analysis we used nanoindentation hardness testing where a diamond tip was indented with equal force into extant and Late Pleistocene bison molar tissues to provide comparative data (17). This showed comparable relative values between fossil and extant teeth (Fig. 3C).

We characterized the hadrosaurid tissue wear properties by subjecting an intact, well preserved *Edmontosaurus* (AMNH 5896) dental battery to micro-tribological wear testing, where

a diamond-tipped probe was drawn across the tooth (1 mm/s, 100 mN normal force) to mimic abrasive feeding strokes (17) (fig. S4). A surface profiler was used to measure the volume of material removed, which was divided by the product of the normal force and sliding distance to reveal the wear rates (17). Indicators that biological values were recovered included correspondence to relief on naturally worn batteries, and the capacity to replicate the chewing surface topography using a three-dimensional tribological simulation (17, 23) based on Archard's wear law (18, 22; see Eq. 1).

$$V (\text{mm}^3) = K (\text{mm}^3/(\text{Nm})) F_n (N) d (m). \quad (1)$$

(Archard's wear Law: wear rate K ($\text{mm}^3/(\text{Nm})$) is the volume of material lost, V (mm^3), per unit of normal load, F_n (N), per distance of sliding, d (m).

The simulation began with a planar surface and ran until the geometry reached an equilibrium state where the combination of contact pressures, which are higher at prominences, and wear resistances resulted in all phases of the materials receding at equal rates. The model was ultimately used to test how tissue distributions and tribological attributes act to create surface features through wear.

To confirm that wear relevant properties are preserved in the 65-69 ma dinosaur fossils we nanoindented teeth from AMNH 5896 and two others (17). Indicators for preservation include: 1) hardnesses correspondent with wear rates, 2) similarity among individuals, and 3) the capacity to predict the chewing surface morphology through the wear model using hardness as a proxy for wear rate (17). We also collected data for the domestic horse (*Equus caballus*) for comparison.

Results show hadrosaurid teeth were composed of six major tissues (Fig. 2D). These include all four wear-relevant constituents that characterize mammalian grinding teeth: enamel

and orthodentine, as well as independently derived secondary dentine and coronal cementum (a tissue used to demonstrate mammalian sophistication [10, 14]). Giant tubules (infilled pulp cavity branches) and a thick mantle dentine are also present. These results suggest that hadrosaurid teeth were among the most histologically complex of any animal (10, 14). Additionally, unlike mammalian teeth (11), tissue distribution varied substantially within each tooth so different configurations were exposed as the teeth migrated transversely across the chewing surface (Fig. 2, D and E). This allowed a single tooth to assume different forms and functions during its progression across the surface of the dental battery (see below).

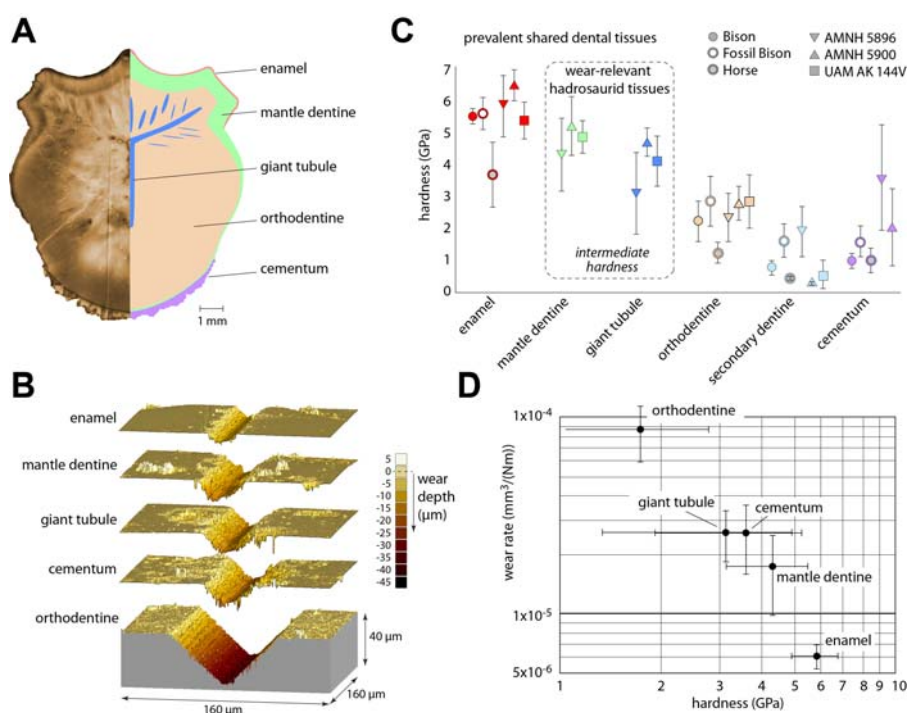


Fig. 3. Wear and hardness characterization. (A) Planarized *Edmontosaurus* tooth with scratch wear track (left). (B) Profilometry of scratched tissues in AMNH 5896. Secondary dentine was not tested owing to its negligible footprint. (C) Mean and standard deviation from nanoindentation experiments on wear relevant tissues in ungulates and hadrosaurids. The fossil bison absolute hardness values appear elevated from degradation of elastic collagen, but relative hardness preservation, critical for understanding wear is evident. Also note that extant ungulate grinding teeth are highly variable in their hardness, even among single tissues, making matches with analogous dinosaur tissues unexpected. (D) Mean wear rates and standard deviation versus the mean hardness and standard deviation for AMNH 5896 tissues.

Testing revealed wear rates ranging from $\sim 90 \times 10^{-6} \text{ mm}^3/(\text{Nm})$ for orthodontine (least wear resistance) to $\sim 6 \times 10^{-6} \text{ mm}^3/(\text{Nm})$ for enamel (most wear resistance) (Fig. 3, A and B), corresponding to observed topographic features on worn batteries (Fig. 1C, 2B). Input of these values into the wear model resulted in identical tooth surface profiles seen in naturally worn batteries including crests where enamel is absent, and branched ridges (Fig. 4). Simulation reveals the contributions of each tissue to the worn topography (fig. S5; see below) and the overall morphology is impossible to achieve without the entire tissue ensemble (figs. S5 and S6).

Nanoindentation revealed mean hardness values from $\sim 2 \text{ GPa}$ for orthodontine to $\sim 6 \text{ GPa}$ for enamel (Fig. 3C). Hardness and wear rates are related as expected for AMNH 5896 (Fig. 3D) and values were similar among *Edmontosaurus* individuals (Fig. 3C). Hardness-based wear models for all three dinosaurs theoretically wore to a morphology matching naturally worn batteries including crests where enamel is absent, and branched ridges (fig. S7).

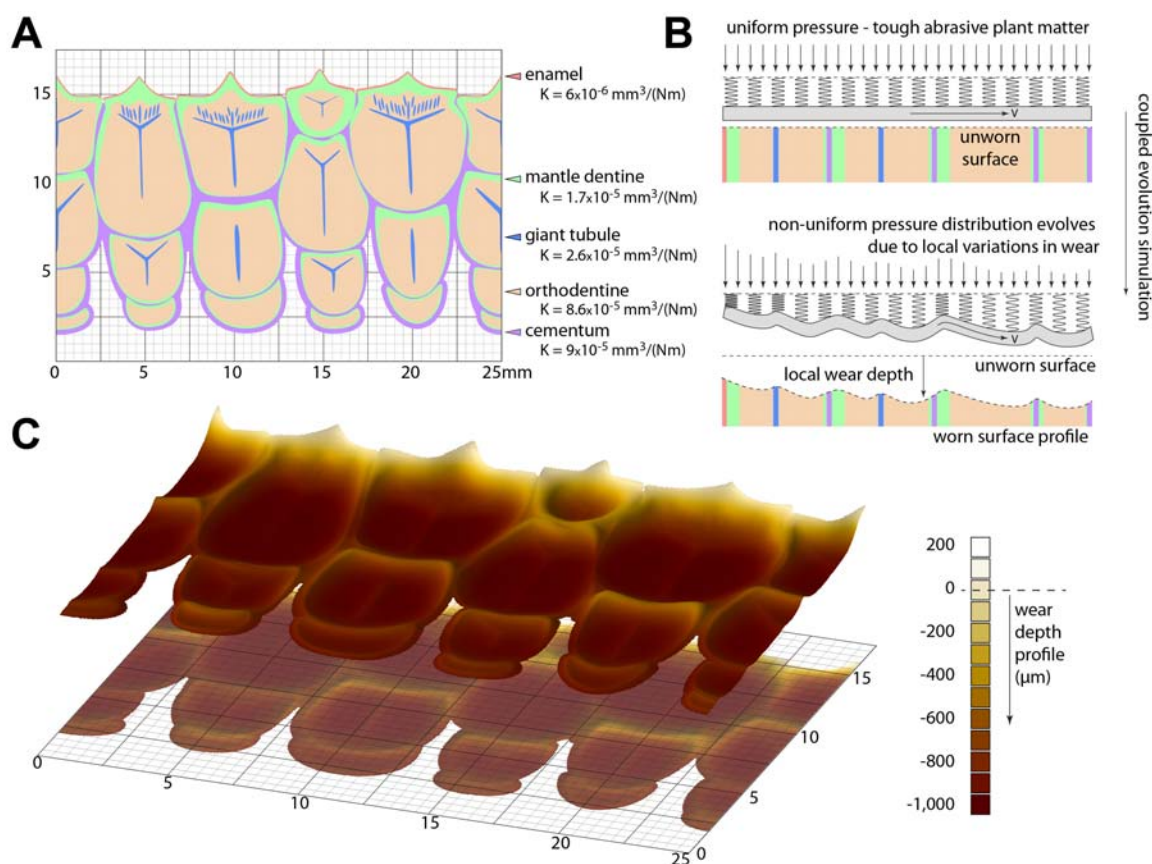


Fig. 4. Tribological modeling of AMNH 5896 dental battery. **(A)** Tissues and measured wear rates used in the simulation. **(B)** Schematic of the computational framework and simulation procedure. An initially flat composite is exposed to abrasive wear under uniform pressure. Progression of wear depth and contact pressure are linked leading to uniform recession only at steady state. **(C)** Equilibrium profile following computational wear modeling of an initially planar composite surface of varying tissue types assigned fossilized wear rate values.

In a phylogenetic context our histological, biomechanical, and simulation data demonstrate how hadrosaurids evolved mammal-like grinding capacity. The primitive condition, seen in *Edmontosaurus* and most taxa (fig. S3) was a dual function slicing-grinding system, presumably for the consumption of fibrous, moderately tough plants (2). The leading teeth have an inclined slicing plane whereas all others form a file-like dental pavement. Highly wear resistant enamel forms crests in all upper battery teeth but only the lead teeth in the lower, since enamel was worn away before the teeth migrated across the chewing surface (Figs. 2A, 4A).

Wear resistant mantle dentine is the tissue that takes over the crest-forming role in the lower batteries (Fig. 4A, fig. S5). The inclined slicing faces in the leading teeth are composed of giant tubule curtains with intermediate wear resistance spanning between the wear resistant mantle dentine crests and the high wear orthodentine basins (Fig. 4A, fig. S5). Large individual and branched giant tubules formed intermediate height ridges partitioning the basins (Fig. 4A, fig. S5). Our modeling shows they influenced basin depth at each tooth position (greater sliding distance = greater scour [22]) and probably provided for finer grinding of plants than major crests (fig. S5). Coronal cementum is prevalent as in mammalian grinding teeth (Figs. 2D, 4A). It similarly served as a bridge minimizing stress singularities on the hard brittle crests, but also acted to bind teeth together (fig. S5). Abscess preventing secondary dentine is present only where the pulp cavity was locally breached, and unlike mammalian grinding teeth, was not a substantial contributor to basin formation through wear.

The distribution of these characters phylogenetically show that longitudinal giant tubules and secondary dentine evolved at the base of Ornithopoda, probably for abscess prevention in association with dental occlusion (fig. S3). The remaining tissues are primitive for Hadrosaurids and evolved as innovations for combined slicing and grinding (fig. S3). Tissue complex modifications appear to have allowed for diversification into specialized ecological niches (fig. S3). Some taxa evolved teeth with coarse grinding pavements across the entire chewing area presumably for the processing of tough plant matter (figs. S2, S3). This was achieved through the loss of transversely oriented giant tubules so slicing plane formation and basin partitioning couldn't occur. In other taxa grinding capacity was completely lost and the teeth were specialized for high-angled slicing (fig. S3). In these batteries transversely oriented giant tubules radiate throughout the teeth so shearing faces formed at all wear stages during migration across the chewing surfaces.

Hadrosaurids evolved the most histologically and biomechanically sophisticated dentitions known among reptiles rivaling those of advanced herbivorous mammals in complexity. Three-dimensional tribological modeling allows for an improved understanding of tissue-level contributions to dental form and function, while tribological properties in fossils allow for direct application throughout vertebrate evolution. Such inferences will be enlightening across major mammalian and reptilian diversifications involving dental/dietary changes (24, 25).

References and Notes

1. V. S. Williams, P. M. Barrett, M. A. Purnell, *Proc. Natl. Acad. Sci.* **106**, 11194 (2009).
2. J. S. Tweet, K. Chin, D. R. Braham, N. L. Murphy, *Palaios* **23**, 624-635 (2008).
3. R. S. Lull, N. E. Wright, *Geol. Soc. Amer. Spec. Paper* **40**, 1 (1942).
4. J. H. Ostrom, *Bull. Amer. Mus. Nat. Hist.* **122**, 1 (1961)
5. D. B. Norman, D. B. Weishampel, in *Biomechanics in Evolution*, J. M. V. Rayner, R. J. Wootton, Eds. (Cambridge Univ. Press, Cambridge, 1991) pp. 161-181.
6. D. B. Weishampel, *Acta Palaeont. Pol.* **28**, 271 (1983).
7. G. M. Erickson, *Proc. Natl. Acad. Sci.* **93**, 14623 (1996).
8. A. Prieto-Márquez, *Zool. J. Linn. Soc.* **159**, 435 (2010).
9. D. C. Evans, C. A. Forster, R. R. Reisz, In *Dinosaur Provincial Park: A Spectacular Ancient Ecosystem Revealed*, P. Currie, E. Koppelhus, Eds. (Indiana Univ. Press, Bloomington, 2005). pp. 349-366.
10. B. Peyer, *Comparative Odontology* (Univ. Chicago Press, Chicago, 1968).
11. S. Hillson, *Teeth* (Cambridge Univ. Press, Cambridge, 1986).
12. C. M. Janis, M. Fortelius, *Biol. Rev.* **63**, 197 (1988).
13. P. L. Lucas, *Dental Functional Morphology: How Teeth Work* (Cambridge Univ. Press, Cambridge, 2004).

14. W. J. Schmidt, A. Keil *Polarizing Microscopy of Dental Tissues*, (Pergamon Press, Oxford, 1971).
15. J. Leidy, *Smith. Contrib. Knowl.* **14**, 1 (1865).
16. R. J. Butler *et al.*, *Proc. Roy. Soc. B.* **277**, 375-381 (2010).
17. Materials and methods are available as supporting material on *Science Online*.
18. J. F. Archard, *J. Appl. Phys.* **24**, 981 (1953).
19. M. M. Khrushchov, *Wear* **28**, 69 (1974).
20. J. D. Currey, R. M. Abeysekera, *Arch. Oral. Biol.* **48**, 439 (2003).
21. W. M. Johnson, A. J. Rapoff, *J. Mater. Sci. Mater. Med.* **18**, 591 (2007).
22. J. F. Archard, W. Hirst, *Proc. R. Soc. Lond. A*, **236**. 397 (1956).
23. W. G. Sawyer, *Tribol. Lett.* **17**, 139 (2004).
24. K. Schwenk (ed) *Feeding: Form, Function and Evolution in Tetrapod Vertebrates* (Academic Press, San Diego, 2000).
25. R. R. Reisz, H. D. Sues, in *Evolution of Herbivory in Terrestrial Vertebrates: Perspectives from the fossil record*, H. D. Sues, Ed. (Cambridge Univ. Press, Cambridge, 2000), pp. 9-41.

Acknowledgements: We thank W. Nix, A. Prieto-Marquez, P. Lee, C. Taylor, E. McCumiskey for their assistance and NSF (EAR 0959029 to GME, MAN) for funding the research. Data can be viewed at: WWW.....

Supplementary Materials

www.sciencemag.org/ tba

Supplementary Text

Figs. S1-S7

Table S1

References (26-40)